Microelectronic Engineering 90 (2012) 92–95

Contents lists available at ScienceDirect

Microelectronic Engineering

journal homepage: www.elsevier.com/locate/mee

Phonon optical modes and electronic properties in diamond nanowires

A. Trejo [a], A. Miranda [a], L. Niño de Rivera [a], A. Díaz-Méndez [b], M. Cruz-Irisson [a,*]

[a] Instituto Politécnico Nacional, ESIME-Culhuacan, Av. Santa Ana 1000, 04430 México D.F., Mexico
[b] Instituto Nacional de Astrofísica Óptica y Electrónica, Luis Enrique Erro # 1, Tonantzintla, Puebla, Mexico

ARTICLE INFO

Article history:
Available online 24 April 2011

Keywords:
Diamond
Nanowires
Tight-binding
Phonons
Raman scattering

ABSTRACT

A local bond-polarization model based on the displacement–displacement Green's function and the Born potential are applied to study the confined optical phonons and Raman scattering of diamond nanowires (DNWs). Also, the electronic band structure of DNWs are investigated by means of a semi-empirical tight-binding approach and compared with density functional theory within local density approximation. The supercell technique is applied to model DNWs along [0 0 1] direction preserving the crystalline diamond atomic structure. The results of both phonons and electrons show a clear quantum confinement signature. Moreover, the highest energy Raman peak shows a shift towards low frequencies respect to the bulk crystalline diamond, in agreement with experimental data.

1. Introduction

The study of nanowires is of current importance both for device applications and fundamental physics being particularly interesting due to their quasi-one-dimensional character [1,2]. Structures such as these are considered to be the building blocks of components for future microelectronic engineering [3]. Diamond nanowires in particular, are attractive due to their remarkable physical properties of highest thermal conductivity in addition to applications in biotechnology and nanomedicine, such as drug delivery [4–8].

It is well-known that phonon properties play an important role in the considered systems because of their significance for the analysis of various physical processes, such as, charge and thermal transport, and optical transitions [9], hence phonon band structures of Si and Ge nanowires have been investigated through DFPT (density functional perturbation theory) [10,11], however there is not such study for diamond nanowires (at the best of our knowledge). The Raman effect in diamond is due to scattering of the light by optical phonons in crystals. Due to the small wavevector of the optical photons, the optical phonon modes in the Raman scattering of crystals have very small momentum compared with the Brillouin zone (BZ). Hence, the phonons involved in first-order Raman scattering have $\mathbf{q} = 0$ and they are at the center of the Brillouin zone (Γ point) [12].

The density functional theory (DFT) is a popular *ab initio* method, since it can be applied to relatively large systems and includes some effects such as electronic correlations and exchange. On the other hand, the semi-empirical approach needs experimental data to define parameters, which usually contain complex many body correlation effects of the system. In addition, the semi-empirical tight-binding (TB) approach has the advantage of being simple and able to handle large supercells.

In the first part of this work, we model the Raman scattering by phonons in DNWs using a local bond polarization model, in which the Green's function, the Born potential, and supercell technique are employed. In the second part, a sp^3s^*-*TB* method is used to study the electronic band structure of DNWs. The results are compared with those obtained from DFT calculations within the local density approximation (LDA).

2. Model and calculation scheme

For modeling DNWs, we start from a cell of eight carbon (c) atoms with side $a = 3.57$ Å, and take periodical conditions only along z-axis, i.e., free boundary conditions are applied in x, y directions, as shown in the inset of Fig. 2(b). C atomic layers are further added in these directions to obtain DNWs with larger cross-sections.

There are several interaction potentials [13,14] able to reproduce the phonon band structure of covalent semiconductors. In order to analyze the phonon confinement effects on the first-order highest-frequency Raman response, it is only necessary to reproduce properly the optical phonon band around the center of BZ. Thus, an interaction potential that describes this condition is the Born model (BM) [15–17]

$$V_{ij} = \frac{1}{2}(\alpha - \beta)\{[\mathbf{u}(i) - \mathbf{u}(j)] \cdot \hat{\mathbf{n}}_{ij}\}^2 + \frac{1}{2}\beta[\mathbf{u}(i) - \mathbf{u}(j)]^2 \quad (1)$$

* Corresponding author.
E-mail address: irisson@unam.mx (M. Cruz-Irisson).

0167-9317/$ - see front matter © 2011 Elsevier B.V. All rights reserved.
doi:10.1016/j.mee.2011.04.052

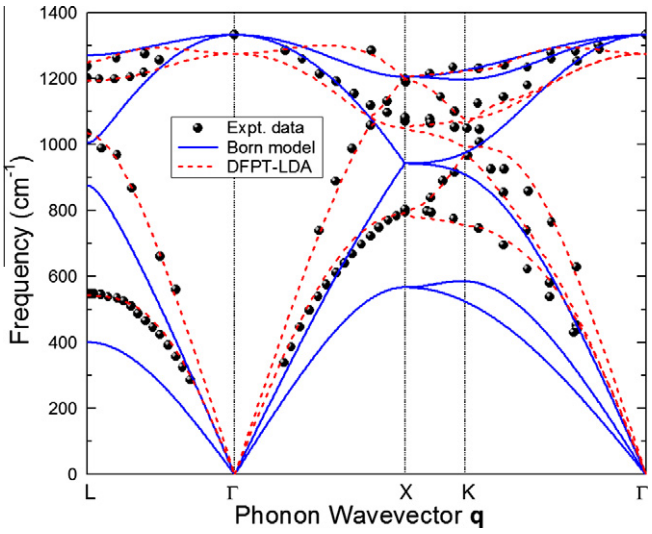

Fig. 1. Calculated phonon band structure within DFPT (dash line) and Born model (solid line) for c-D and compared with experimental data (spheres) from Ref. [23].

where $\mathbf{u}(i)$ is the displacement of atom i with respect to its equilibrium position, α and β are respectively central and non-central restoring force constants which are obtained by comparing the theoretical phonon dispersion relationship with the inelastic neutron scattering data [18]. The unitary vector $\hat{\mathbf{n}}_{ij}$ indicates the bond direction between atoms i and j. This interatomic potential has the advantage of containing only two parameters, and reproduces the optical phonon band of bulk crystalline diamond (c-D) around the center of BZ, as shown in Fig. 1 (solid line). The Dyson equation for the Green's function ($\mathbf{G}$) can be written by [19]

$$(M\omega^2\mathbf{I} - \Phi)\,\mathbf{G}(\omega) = \mathbf{I} \tag{2}$$

where M is the atomic mass of C, $\mathbf{I}$ stands as the identity matrix, and Φ is the dynamic matrix, whose elements are given by

$$\Phi_{\mu\mu'}(i,j) = \frac{\partial^2 V_{ij}}{\partial u_\mu(i)\partial u_{\mu'}(j)} \tag{3}$$

with $\mu, \mu' = x, y,$ or z.

On the other hand, Raman scattering study is a powerful tool for investigating the composition, bonding, and structural properties of nanostructures [20]. However, the fundamental electronic processes involved in the Raman scattering (RS) are complicated to describe theoretically because it involves photons, electrons, and phonons.

Within the local bond polarization model and the linear response theory, the Raman spectrum $[R(\omega)]$ can be calculated by [21,22]

$$R(\omega) \propto \omega \mathrm{Im} \sum_{\mu,\mu'} \sum_{i,j} (-1)^{i-j} G_{\mu\mu'}(i,j,\omega) \tag{4}$$

where i and j are the atoms index, and the Green's function $[G_{\mu\mu'}(i,j,\omega)]$ is defined in Eq. (2).

For the electrons case, the surface dangling bonds are saturated with H atoms where H–C bond length is 1.098 Å [23]. In TB approximation, sp^3s^* is a basis that reproduces the indirect band-gap of diamond. The parameters of Vogl and co-workers [24], which reproduce an indirect-gap of 5.47 eV for c-D are used. In addition, a study of CH_4 leads to an H on-site energy of -4.049 eV and hopping integrals between H and C are $ss\sigma_{H-C} = -4.81$ eV and $sp\sigma_{H-C} = 5.32$ eV [23]. The electronic states of DNWs are determined by diagonalizing the TB Hamiltonian matrix.

The DFT calculations for the electronic structure of DNWs were performed using the LDA [25] with ultrasoft Vanderbilt pseudopotentials [26] as implemented in the CASTEP code [27] within the Materials Studio software suite. All DNWs are optimized through the BFGS algorithm [28] considering that the local minimum is achieved when the maximum residual forces on the atoms are less than 0.03 eV/Å. A cutoff energy of 280 eV is used. The BZ has been sampled using grids up to $1 \times 1 \times 4$ according to the Monkhorst–Pack scheme [29] for the electronic minimization and geometry optimization, while grids up to $1 \times 1 \times 7$ were used for Density of States (DOS) calculations.

3. Results

Calculations of the phonon band structure were carried out using the parameters $\alpha = 357.0\ \mathrm{Nm^{-1}}$ and $\beta = 57\ \mathrm{Nm^{-1}}$. In Fig. 1 the phonon band structure calculated within the BM (solid line) and DFPT (dash line) are compared with experimental data (spheres) for c-D [18]. Note that the calculated highest frequency optical mode within DFPT is located at $\omega_0 = 1275\ \mathrm{cm^{-1}}$ while the obtained by BM is $1332.39\ \mathrm{cm^{-1}}$ which is close to the experimental value of $1332\ \mathrm{cm^{-1}}$ [18]. The good agreement between theory and experiment highlights the accuracy of the BM only around the Γ point. This optical mode is Raman active. Hence we have chosen this approach to study the optical phonon modes and RS in DNWs.

Fig. 2(a) and (b) shows, respectively, the phonon band structure and Raman response of DNW with a cross section of $d = 0.357$ nm. Observe that there are several peaks in the Raman response spectrum and the highest frequency peaks has a shift toward lower frequencies in comparison with the c-D case. This increased number of Raman active modes at the Γ point, as shown in Fig. 2(b), is directly related to the employment of the supercell technique being consequence of the first BZ folding.

To have a better understanding of the variation of the highest frequency optical modes as a function of the width of the DNWs, we also calculated the corresponding Raman shift; including an imaginary part in the energy of $0.1\ \mathrm{cm^{-1}}$. In Fig. 3, the highest-frequency Raman shift is plotted as a function of the cross-section length (d) for DNWs with rhombic shapes. The inset of this figure shows the calculated Raman peak of c-D at $1332\ \mathrm{cm^{-1}}$, very close to the experimental data which reports the peak at $1332.79\ \mathrm{cm^{-1}}$ [30]. Also the maximum Raman shifts of DNWs with $d = 0.88$ and 0.5 nm are shown. Notice that the variation of these Raman peaks to lower energies is observed in DNWs samples [31], in spite of the peak broadening is not being reproduced, probably due to the ab-

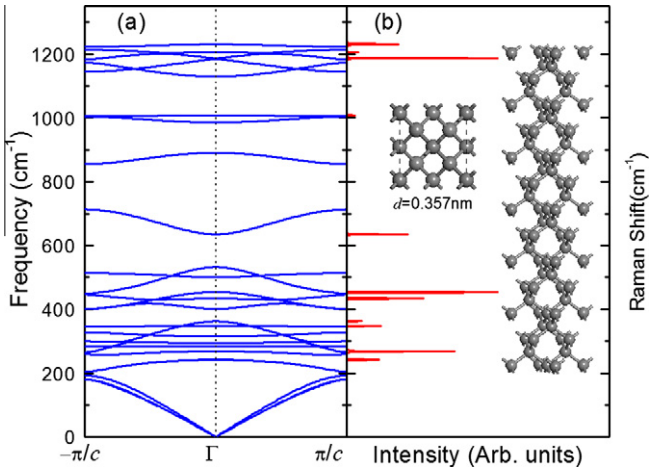

Fig. 2. (a) Phonon band structure and (b) Raman response for a DNW with width $d = 0.357$ nm. Inset: Nanowire top and side view.

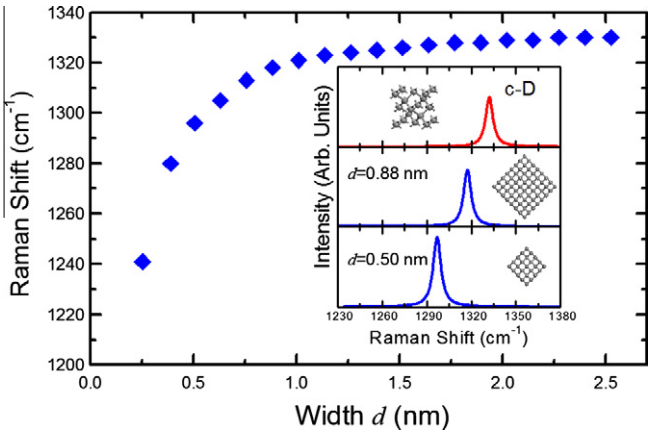

Fig. 3. Raman response calculated by Eq. (3) for DNWs as function of d. Inset: The main Raman peak for crystalline diamond (c-D) and DNWs with $d = 0.88$ and 0.5 nm.

sence of the laser heating effects as well as inhomogeneous diameters of DNWs. However, this shift shows a clear quantum confinement effect. Observe that the highest frequency Raman peak of quantum wires tends asymptotically to the c-D value ($\sim$1332 cm^{-1}), when the transversal cross section of the wires increases.

In the following, we will describe the electronic properties of H passivated, free standing diamond nanowires oriented along [0 0 1] direction with widths ranging from 0.25 to 2.52 nm, contained in corresponding supercells from 9 to 441 carbon atoms. Fig. 4(a–d) shows the electronic band structure of c-D and DNWs, obtained from TB (blue lines) and DFT–LDA (orange area) calculations. For c-D, a primitive unitary cell of two C atoms is used. Notice the good agreement between *ab initio* and semi-empirical TB results around the valence band maximum (VBM). Observe that LDA underestimates de band gap energy.

The calculations of electronic band structure from TB for DNWs with $d = 0.50$, 0.37, and 0.25 nm have been solidly shifted by $\delta = 4.58$, 3.43, and 2.69 eV, respectively in order to adjust its VBM energy to the DFT–LDA one. It can be seen that the good agreement continues for the VBM but the LDA band gap underestimation becomes greater when reducing size of DNWs. It is worth to observe that DFT–LDA band gap is always direct. Meanwhile, the TB one is indirect for all cases. The difference between the conduction bands

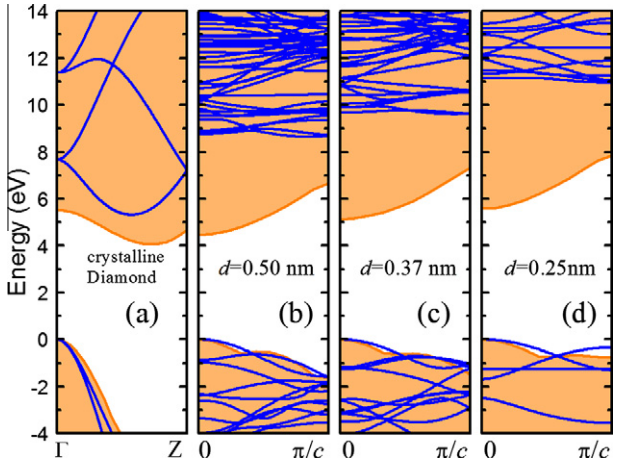

Fig. 4. Electronic band structure for: (a) c-D and (b–d) DNWs calculated from TB (blue lines) and DFT–LDA (orange area). (For interpretation of the references to color in this figure legend, the reader is referred to the web version of this article.)

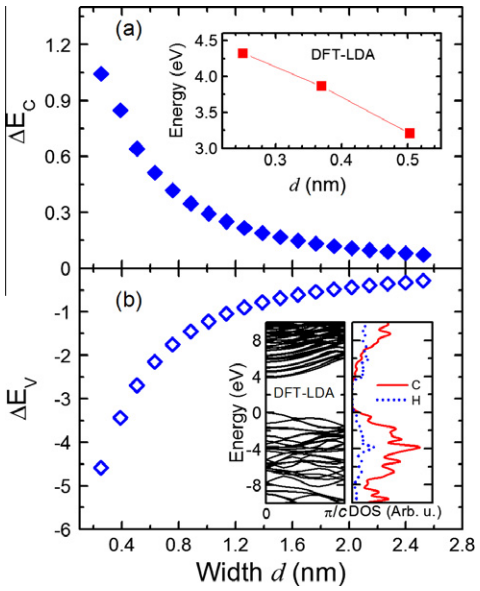

Fig. 5. The edge enlargement of: (a) valence band (ΔE_v) and (b) conduction (ΔE_c) band as a function of width d. Inset (a): Energy band gap of DNWs obtained from DFT–LDA (red rhombus). Inset (b): Electronic band structure and projected DOS from DFT–LDA for a DNW with $d = 0.38$ nm. (For interpretation of the references to color in this figure legend, the reader is referred to the web version of this article.)

could be due to that the s^* orbital has non d-wave symmetry and additionally the geometry optimization is absent in the TB calculations. However, in both approaches the band gap show a clear broadening due to quantum confinement.

The edge enlargement of VBM, defined as the difference between DNWs and c-D VBM [$\Delta E_v = E_v(d) - E_g^v(\infty)$], versus the width ($d$) of nanowire is plotted in Fig. 5(a) as empty rhombus. In similar form Fig. 5(b) shows the enlargement of the edges of conduction band minimum (CBM) [$\Delta E_c = E_c(d) - E_g(\infty)$] illustrated by solid rhombus. Observe that the band edges move away and approach asymmetrically as the width decrease and increase, respectively. This asymmetry is originated from the difference of electron and hole effective masses in c-D.

The calculations of energy band gap from DFT–LDA for three different DNWs widths are plotted in the inset of Fig. 5(a). Notice the almost linear decrease in the band gap when the width is increasing. Additionally, in the inset of Fig. 5(b) we show the electronic dispersion relation for a nanowire with $d = 0.37$ nm. The projected DOS in the right panel illustrates the contribution of the surface dangling bond H passivation. Notice the important contribution of hydrogen atoms to the electronic states around the CBM.

4. Conclusions

We have presented a microscopic theory to model the phonon optical modes and Raman scattering in DNWs, by using a very simple interaction potential that includes only two parameters which simulate stretching (central) and bending (non-central) vibrational modes. The results show that the highest-frequency Raman peak shifts to lower frequencies as the nanowire width increases, due to phonon confinement, in concordance with the experimental data. On the other hand the electronic structure calculations show a disagreement between the DFT and TB approaches in both the nature and the size of the energy band gap. However, for the two cases the band gap enlargement with decreasing size of diameters

of nanowires according to the quantum confinement scheme is observed.

Finally, Raman response as well as TB electronic band gap of DNWs show a consistent asymptotical behavior to the bulk crystalline limit when the width of wires enlarges.

Acknowledgments

This work was supported by Projects SIP-IPN: 20090652 and SIP-IPN: 20101142. The computing facilities of DGSCA-UNAM are fully acknowledged.

References

[1] O. Hayden, R. Agarwal, W. Lu, Nanotoday 3 (2008) 12–16.
[2] V. Dřínek, R. Fajgar, M. Klementová, J. Šubrt, J. Electrochem. Soc. 157 (2010) K218–K222.
[3] M. Najmzadeh, L. De Michielis, D. Bouvet, P. Dobrosz, S. Olsen, A.M. Ionescu, Microelectron. Eng. 87 (2010) 1561.
[4] B.J.M. Hausmann et al., Diamond Relat. Mater. 19 (2010) 621.
[5] J.-I. Chao et al., Biophys. J. 93 (2007) 2199.
[6] R. Lam, M. Chen, E. Pierstorff, H. Huang, E. Osawa, D. Ho, ACS Nano 2 (2008) 2095.
[7] C. Bradac, T. Gaebel, N. Naidoo, J.R. Rabeau, A.S. Barnard, Nano Lett. 9 (2009) 3555.
[8] A. Adnan et al., Mol. Pharm. 8 (2011) 368.
[9] G.P. Srivastava, The Physics of Phonons, Taylor and Francis Ltd., London, GB, 1990.
[10] H. Peelaers, B. Partoens, F.M. Peeters, Nano Lett. 9 (2009) 107.
[11] H. Peelaers, B. Partoens, F.M. Peeters, Appl. Phys. Lett. 95 (2009) 122110.
[12] A.K. Arora, M. Rajalakshmi, T.R. Ravindran, V. Sivasubramanian, J. Raman Spectrosc. 38 (2007) 604.
[13] P.N. Keating, Phys. Rev. 145 (1966) 637.
[14] F.H. Stillinger, T.A. Weber, Phys. Rev. B 31 (1985) 5262.
[15] V.J. Torres, A.M. Stoneham, Handbook of Interatomic Potentials III, Semiconductors, Atomic Energy Research Establishment, Harwell, England, 1985.
[16] P. Alfaro, M. Cruz, C. Wang, IEEE Trans. Nanotechnol. 5 (2001) 466.
[17] P. Alfaro, M. Cruz, C. Wang, Nanoscale Res. Lett. 3 (2008) 55.
[18] J.L. Warren, J.L. Yarnell, G. Dolling, R.A. Cowley, Phys. Rev. 158 (1967) 805.
[19] R.J. Elliott, J.A. Krumhansl, P.L. Leath, Rev. Mod. Phys. 46 (1974) 465.
[20] G. Gouadec, P. Colomban, J. Raman Spectrosc. 38 (2007) 598.
[21] R.M. Martin, F.L. Galeener, Phys. Rev. B 23 (1981) 3071.
[22] P. Alfaro, R. Cisneros, M. Bizarro, M. Cruz-Irisson, C. Wang, Nanoscale 3 (2011) 1246.
[23] M.D. Winn, M. Rassinger, J. Hafner, Phys. Rev. B 55 (1997) 5364.
[24] P. Vogl, H.P. Hjalmarson, J.D. Dow, J. Phys. Chem. Solids 44 (1983) 365.
[25] D.M. Ceperley, B.J. Adler, Phys. Rev. Lett. 45 (1980) 566.
[26] D. Vanderbilt, Phys. Rev. B 41 (1990) 7892.
[27] S.J. Clark et al., Zeits Krist. 220 (2005) 567.
[28] B.G. Pfrommer, M. Côté, S.G. Louie, M.L. Cohen, J. Comp. Phys. 131 (1997) 233.
[29] H.J. Monkhorst, J.D. Pack, Phys. Rev. B 13 (1976) 5188.
[30] M. Yoshikawa, Y. Mori, M. Maegawa, G. Katagiri, H. Ishida, A. Ishitani, Appl. Phys. Lett. 62 (1993) 3114.
[31] K.W. Sun, J.Y. Wang, T.Y. Ko, Appl. Phys. Lett. 92 (2008) 153115.